EFFECTS OF FIREWORKS ON THE AIR QUALITY IN BUDAPEST

Diploma Thesis

Master of Science in Chemistry

FELIPE REIS FERNANDES

Supervisor: Dr. Salma Imre

Department of Analytical Chemistry

ELTE Eötvös Loránd University, Budapest

Institute of Chemistry

Faculty of Science

Defense taking place at the Department of Analytical Chemistry

2022

Contents

List of Abbreviations

AT	After-Time, from 22:30 to 23:30 on 20th August of every year
BpART Lab	Budapest platform for Aerosol Research and Training Laboratory
BT	Before-Time, from 20:00 to 21:00 on 20th August of every year
CPC	Condensation Particle Counter
DMPS	Differential Mobility Particle Sizer
DT	During-Time, from 21:08 to 22:00 on 20th August of every year
ELTE	Eötvös Loránd University
$N_{6–25}$	Particle number concentration, in the diameter range between 6 and 25 nm
$N_{6–100}$	Particle number concentration, in the diameter range between 6 and 100 nm
$N_{6–1000}$	Particle number concentration, in the diameter range between 6 and 1000 nm
$N_{100–1000}$	Particle number concentration, in the diameter range between 100 and 1000 nm
NW	North–West
PAH	Polycyclic aromatic hydrocarbon
PM	Particulate Matter
PM_{10}	Particulate Matter with aerodynamic diameter less than or equal to 10 µm
$PM_{2.5}$	Particulate Matter with aerodynamic diameter less than or equal to 2.5 µm
RH	Relative Humidity
RDiff	Relative Difference
T	Air Temperature
WD	Wind Direction
WS	Wind Speed

1 Introduction and objectives

The origin of fireworks is directly related to the invention of gunpowder. The first fireworks were created in China during the Song dynasty that lasted from 960 to 1279 (Gernet 1962, Ball 1925). Fireworks were largely used during many festivals for amusement (Temple, 2007). Later in Europe fireworks were a significant element of early modern life. The fire and light could make a strong impression on the overall population. Between the 14th and 19th centuries, several communities displayed their power with demonstration of control over the fire, in artificial fireworks exploding around allegoric scenarios and important landmarks, natural like rivers or manmade such as bridges (Werret, 2010).

In the 17th century the popularity of fireworks in Europe scaled up considerably (Griffiths et al., 2017). In 1786 Bertholet discovered that K salts in fire resulted in an emission of light in violet color. Later it was found that the burning of chlorates of other elements such as Ba, Sr, Cu and Na also resulted in intense bright colorful emissions. These series of discoveries together with a further use of metallic Al and Mg that produce silvery lights contributed considerably to the possibilities for creation of fireworks (Griffiths et al., 2017).

In present Hungary, one of the most prominent use of fireworks happens on 20th of August, during the celebration of the Saint Stephen's Day. Stephen (István in Hungarian) was born in 969 and died in 1038 (Cartledge, 2011). He was Hungary’s first king, and he laid the foundation of the state by converting the nomad and pagan Magyar people (Hungarians) into Christianity (Berend et al., 2007). The Celebration occurs almost every year and in Budapest the grand finale is marked by a 30-minute-long firework show along the Danube promenade (Kató and Kató, 2014, 2015, 2016, 2017). At the same time, fireworks influence the air quality on a local scale and for a brief time. Since many spectators gather around the site of the event and the area surrounding it is a densely populated urban area, it is relevant to study the effects of fireworks on the air quality.

The main goal of this work was to characterize the air pollution generated by the firework spectacle in Budapest during Saint Stephen's day retrospectively for several years. Special attention was given to the 2021 celebration since it was reported to be the most extensive over the years in Europe. The analysis was mostly focused on the particulate matter, particle number concentration,

particle size distribution and their changes in comparison with the usual conditions for the same location. The possible influence of meteorological conditions was also evaluated.

From the individual perspective this work has allowed the study of the aerosol concentration behavior, a deeper understanding of the phenomena involved and the building of the scientific method towards understanding a particular event, which in this case were fireworks. My own work included the review of the literature background from a historical and chemical perspective of fireworks, the study of phenomena related to how aerosol particles of different sizes can relate to each other, and the verification of hypotheses raised by other authors using our data. Besides that, there was a fantastic opportunity to learn about the operational principles and methods used in aerosol science. Working with time series data and performing exploratory statistical analysis, creating Python scripts to handle and organize the data collected, merging different datasets, performing corrections and respective data visualization creation were an important part of the initial work. Finally, the merging of all analysis made, exposition of the results, analysis and drawing conclusions as well as further questions which were all placed within this thesis as well the corrections and consultations completed all the efforts and learnings related to this work. The performed work is part of and contributes to the activities in the Budapest platform for Aerosol Research and Training.

2 Literature background

2.1 Chemical perspective

Apart from the historical and cultural aspects, firework events are also a known source of pollution, in particular for aerosol. The metals applied on firework manufacturing are usually related to the color they produce. Red, green, and blue are given by Sr, Ba and Cu, respectively (Perry, 1999; Kulshrestha et al., 2004; Wang et al., 2007; Moreno et al., 2007). A firework article is a small pyrotechnic missile that explodes in the air and creates bursts of brightly colored light and sudden loud sound effects. It contains 1) propellant and fuel, 2) oxidants and 3) metals whose electron excitation at elevated temperatures of the deflagration yields the colored displays (Russell, 2009; Sun et al., 2017; Cao et al., 2018). The first group classically contains C (in forms of carbon black, sugar, or starch), elemental S and P, and possibly some fuel metals such as Mg, Al, Fe and Zn. The oxidants are made of nitrates, perchlorate, chlorates, or hydrogen terephthalate salts (of K), which support the detonation of the fuel. The last group if ingredients includes Li, Na, Al, Ca, Ti, Fe, Co, Cu, Zn, Sr, Ba and Pb compounds (Russell, 2009; Hickey et al., 2020). They generate various colors, for instance, Sr red, Ba green, Cu blue, Ca orange, Li pink and Na yellow (Lin, 2016). Sometimes the same substance is used to provide color and oxygen or for stabilizing the mixture. Further compounds are added for dedicated functions such as organic dyes for smoke generation, Ti to enhance the production of sparks, metal salicylates for noise effects and chlorinated organics for color enhancement or deepening.

The deflagration of fireworks is a source of pollutants like O_3, SO_2, and NO_x (Attri et al., 2001; Ravindra et al., 2001), CO, aerosol particles which contain heavy and transition metals (Wang et al., 2007). Particles contain Ba, Cu, Mg, K, and Sr, organic carbon, and some secondary compounds such as nitrates and organic substances (Kulshrestha et al., 2004; Drewnick et al., 2006; Moreno et al., 2007; Wang et al., 2007). Firework episodes can lead to considerable increase of metals less commonly found in atmosphere for instance: 120 times increase in Sr, 22 times in Mg, 12 times in K, 11 times in Ba and Cu (Vecchi et al., 2008). Besides aerosol, there is evidence of other toxic organic compounds like octachlorinated dioxins, furans and hexachlorobenzene in the firework remains (Fleischer et al., 1999).

The measurement of aerosol concentration in the atmosphere is mostly done with two different parameters, particulate matter mass and particle number. The first and most common is

the particle mass which considers the mass of particles per volume of air and mostly this is subdivided depending on the size ranges of particles. The classification PM_{10} mass refers to the total mass of particles with diameter equal to or smaller than 10 µm per volume of air. Particle number on the other hand focus on the number of particles within an equivalent diameter per volume of air. Different equivalent diameters can be measured within one piece of equipment if adjusted to capture different sizes. The equivalent diameter depends on different particle behavior or characteristics, like the aerodynamic given by the particle inertia and the gravity or the electrical mobility given by the electrically induced motion of the particle. In this study the particle number was measured using the electrical mobility of particles.

2.2 Effects on air quality

Hourly peaks above 1000 µg m^{-3} PM_{10} mass were measured during the Chinese New Year (Lai and Brimblecombe, 2017) and Diwali Festival in India (Peshin et al., 2017). Extraordinarily elevated levels of pollution related to fireworks were also found in many other events like the Guy Fawkes in England (Pope et al., 2016), Independence Day in the United States (Seidel and Birnbaum, 2015), sport events and new year celebrations in many countries. Even so, such celebrations do not last for a long time and higher concentrations of particulate matter remain in the air for a few hours. There are, however, health concerns related to the increased aerosol levels (Yao et al., 2019). This short-term pollution episodes often remain unnoticed for most monitoring stations (Gonzales et al., 2017), even though it contributes significantly to metal emissions (Moreno et al., 2007) and urban background trace metals (Moreno et al., 2010). If the particles are deposited on environmental surfaces, the foulant can pollute the surface waters, soil, and dust for a longer time (Baranyai et al., 2015). Perchlorate pollution of waters was already reported (Scheytt et al., 2011).

The exposure to air pollution at lower levels than previously reported had led to adverse effects according to more recent epidemiological studies (WHO, 2021). In the most recent Air Quality Guideline (AQG) released by the World Health Organization (WHO), the average concentration in 24 hours for $PM_{2.5}$ mass should be bellow 15 µg m^{-3} and for PM_{10} mass bellow 45 µg m^{-3}. When we compare such values as the ones found by Lai and Brimblecombe (2017) for example, we can see the potential hazard fireworks might have for human health.

Another aspect to be considered for aerosol pollution is the ultrafine (UF) particles which are particles with equivalent diameter less or equal to 100 nm. Following the most recent WHO guidelines, it is becoming a consensus that concentrations below 1000 cm^{-3} (24-hour mean) can be considered as low. It is proposed that 24-hour mean concentrations exceeding 10 000 cm^{-3} or 1-hour mean concentrations exceeding levels of 20 000 cm^{-3} can be considered high (WHO, 2021). Advantages of UF particle measurement are the relatively short atmospheric residence time of the particles which allow the identification of active sources with results less affected by the atmospheric transformation processes.

2.3 Aerosol from fireworks

The particles produced have a metallic and strongly inorganic characteristic and the particle average size is around 1.2 μm (Liu et al., 1997). Less commonly researched, however, is the size distribution of the aerosol particles as well as their evolution related to time. Some studies suggest that during firework events there is an increase in Aitken mode (Jing et al., 2014; Zhang et al., 2010; Zhao et al., 2017; Joshi et al., 2016), other researchers have documented a significant increase in UF particles during fireworks (Wen and Chen, 2013; Joshi et al., 2016). Nonetheless, most experiments were unable to present any conclusive evidence in differentiating a firework episode and a normal event mainly because of the influence of other anthropogenic emissions and due unavailability of the aerosol chemical composition. Additionally, some other studies for Diwali festival India and Chinese New Year in China (Yadav et al., 2019; Li et al., 2016) have found an initial increase in UF particles followed by physical aging process resulting in particle growth.

The temporal characteristics of aerosol formation in fireworks are the brief time when the process happens, on each explosion, and the short time of the spectacle itself. Collection of aerosol samples is challenging due to the narrow time window available for sampling, reflecting also on the detection of the metals used in the fireworks. To understand firework phenomenon, it is more suitable to have an online measurement method capable of capturing the immediate change in the aerosol concentration, detecting the decline in the concentration of the same due to the short residence time in atmosphere of the particles and at different particle sizes. To fit all these characteristics, elucidate the size distribution and understand if there were transitions between particle sizes in this study the online monitoring of the particle count concentration was chosen as the main measurement for characterization of the firework events.

2.4 Health effects of firework smoke

The main concern regarding the pollutants emitted during firework events is their effect on human health (Baranyai et al., 2015). Even considering that the longest events are limited to festivals of a few days and mostly of spectacles ranging from just minutes to hours, their impact cannot be ignored. Fireworks have the potential to increase the concentration of certain pollutants several times about the safety levels for a brief time span. The acute exposure to high concentrations of PM, transition metals and carcinogens can lead to issues ranging from mild respiratory symptoms to death (Curtis et al., 2006).

Particulate Matter inhalation from fireworks was reported to lead to lower respiratory symptoms (Beig et al., 2013). Respiratory chronic diseases such as asthma and chronic obstructive pulmonary disease seem to be worsened by firework pollution (Gouder et al., 2014). Some pollutants such as SO_2 can be transported to the deepest parts of the respiratory tract leading to long-term effects. Lung damage from NO_2 can happen even for acute exposure (Ambade et al., 2013). Dyspnea and pneumonia may be caused by O_3 and CO (Gouder et al., 2014). The metals from fireworks, mainly Cd, Cr, Ni and Pb, are known human carcinogens and might be associated with lung cancer (Verougstraete et al., 2003; Pearson et al., 2005; Moreno et al., 2010). The heavy metals and PAHs in the particles can also increase non-carcinogenic and carcinogenic risks to health especially through respiratory and dermal contact.

Besides the biochemical risks, fireworks can lead to physical explosion injuries from trauma, burns and noise-induced hearing loss (Brookhouser et al., 1992; van Kamp et al., 2005). All these risks accumulated make it important to understand and control the firework spectacles.

3 Methods

3.1 Time intervals considered

The data of our analysis corresponds to the years 2009, 2014, 2015, 2016, 2017, 2020 and 2021. The years from 2010 to 2013 were not evaluated as the measurement devices utilized for the study were at a further and different location in Budapest. In 2018 and 2019, due to some water condensation transient troubles the measurements were not available. On 2020 Due to the coronavirus pandemic restrictions there was no spectacle. On the event days the focused time span was from 20:00 to 23:30 considering that all years the fireworks took place on 20th August and started close to 21:00 (with eventual few minutes delay on some years) and the spectacle varied between 25 and 35 minutes.

The comparison of the measurements was made by taking as basis the time before, during and after the firework events. The Before-Time was considered from 20:00 to 21:00, the During-Time was considered from 21:00 to 22:00 and finally the After-Time, was the time range from 22:30 to 23:30. The 30-minute gap between the During-Time and the After-Time was established as it was an interval with characteristics of both a time with fireworks and without fireworks which could compromise the quality of the data analyzed. Also, the during time was not considered sharply at 21:00 but at 21:08 due to the usual firework event introduction time as well as to avoid the influence on the average data from a time before the firework events start given the time resolution of 8 minutes of the main equipment used on the measurements.

In 2021, the year of reference for firework events, the spectacle was not fully continuous. The event happened in 7 blocks with drones and music in between. The pauses were also selected to improve the visibility during the show. Something similar happened on the other years, however we could not gather precise details on the timings of the explosions besides their programmed start and end.

3.2 Location

In all years analyzed the fireworks happened along the Danube River in central Budapest. Each year there were variations on the exact area which was delimited by the bridges of the city, the number of effects used and the exact disposition of the charges (if on riverbanks, middle of the river and on the bridges) also varied. A summary of the areas over the river where the fireworks

were, the number of effects, the bridges delimiting the area, the time of the spectacle is given in Table 1. The areas of the event were calculated with the free area calculation tool available on Google Maps.

Table 1: Overview of the firework events each year. An indication of the available experimental collection is also provided. N.A. stands for not available.

Year	Start (HH:mm)	Duration (min)	N° effects	Area limits (area of interest between the bridges)	Event area (km^2)	Measurement Available
2009	21:00	20	6000	Margareth – Elizabeth	1.0	Yes
2010	21:00	30	N.A.			No
2011	21:00	30	N.A.			No
2012	21:00	30	N.A.			No
2013	21:00	25	N.A.			No
2014	21:00	30	11000	Margareth – Petőfi	1.5	Yes
2015	21:00	30	10000	Széchenyi – Liberty	0.5	Yes
2016	21:00	30	21000	Széchenyi – Elizabeth	0.3	Yes
2017	21:00	30	25000	Margareth – Széchenyi	0.6	Yes
2018	21:00	30	21000	Margareth – Elizabeth	1.0	No
2019	21:00	30	26000	Széchenyi – Elizabeth	0.3	No
2020				No firework		Yes
2021	21:05	35	40000	Margareth – Petőfi	1.5	Yes

The location and area of the fireworks on 2014 and 2021 are shown in Figure 1. An example of the disposition of the firework charges for 2021 can be seen in Figure 2.

Figure 1: Aerial view of central Budapest with the Danube River crossing it. Surrounded by the red line is the largest area (corresponding to the events of 2014 and 2021) where the fireworks happened. The yellow dot represents the BpART Laboratory.

The measurements were done at the Budapest platform for Aerosol Research and Training (BpART) Laboratory (47° 28' 30" N, 19° 3' 45" E; 115 m above the mean sea level). Its rooftop level is located at a height of 11 m above the street of the closest road. The distance of the container from the right bank of the river Danube is approximately 85m (Salma et al., 2016b). The location of the laboratory is especially suited for the measurements due to the relative proximity to the firework area and riverbank. Besides that, the major wind flow in the city is NW (Salma et al., 2016a) and the firework events center area is around NW of the lab location. There were no regular monitoring stations of the National Air Quality Monitoring Network (OLM) in the adjacent area.

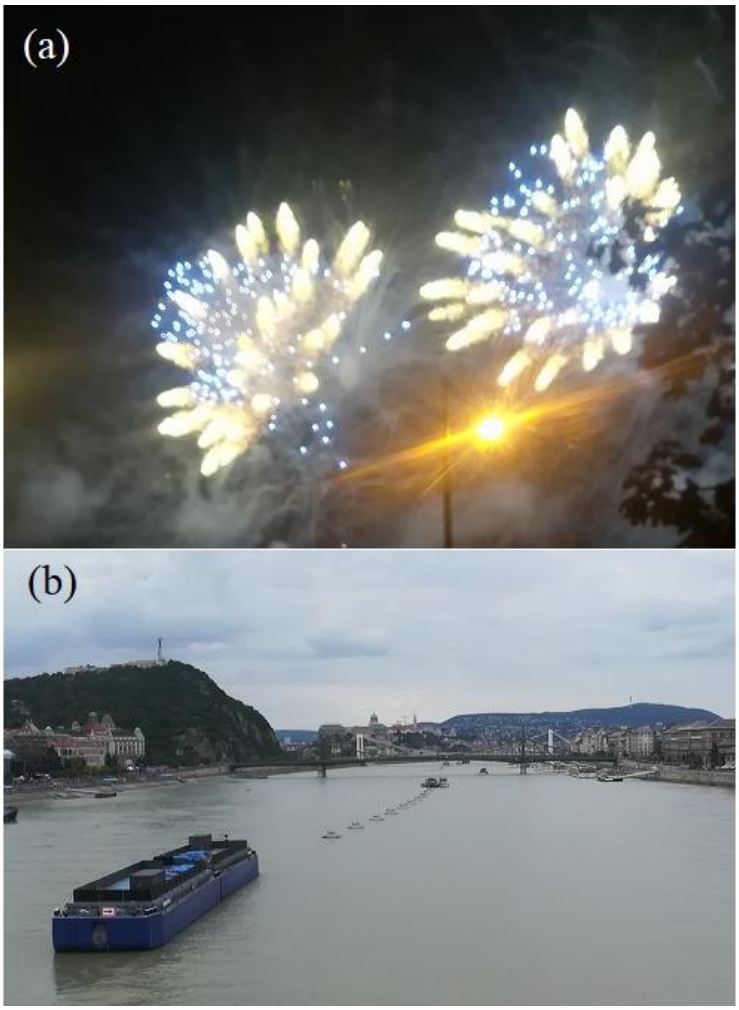

Figure 2: The fireworks (a) where the smoke produced by the event can be seen beside the light spectacle. Center of Budapest with the Danube River with the firework charges placed on boats (b). Both pictures were taken by the author on 20th August 2021.

3.3 Measurements

Particle number size distributions and total particle number concentrations were measured by differential mobility particle sizer (DMPS) and condensation particle counter (CPC), respectively. These were complemented by meteorological properties. All the measurements were realized at the BpART Laboratory. They are normally in continuous operation and the related experimental data were extracted from the larger data sets.

3.3.1 Differential mobility particle sizer

The concentrations of particle number (*N*) and its fractions were determined by a flow-switching-type differential mobility particle sizer (DMPS). It measured particle number concentrations in the electrical mobility diameter range from 6 to 1000 nm in the dry state (with RH < 30 %) in 30 channels with a time resolution of 8 min (Salma et al., 2011a, 2016). Its main components included a radioactive ($_{60}$Ni) bipolar diffusion charger, a Nafion semipermeable membrane monotube dryer, a 28-cm-long Vienna-type differential mobility analyzer (DMA) and a butanol–based CPC (TSI, model 3775, USA). The aerosol flow rates in the high and low modes were 2.0 and 0.31 L min^{-1}, respectively. The sheath flows were 10 times larger than the aerosol flows. The sampling inlet was made of copper tube with a diameter of 6 mm and a length of around 1.9 m. The measurements were realized semi-continuously according to international technical standards (Wiedensohler et al., 2012). The DMPS system used can be seen on Figure 3.

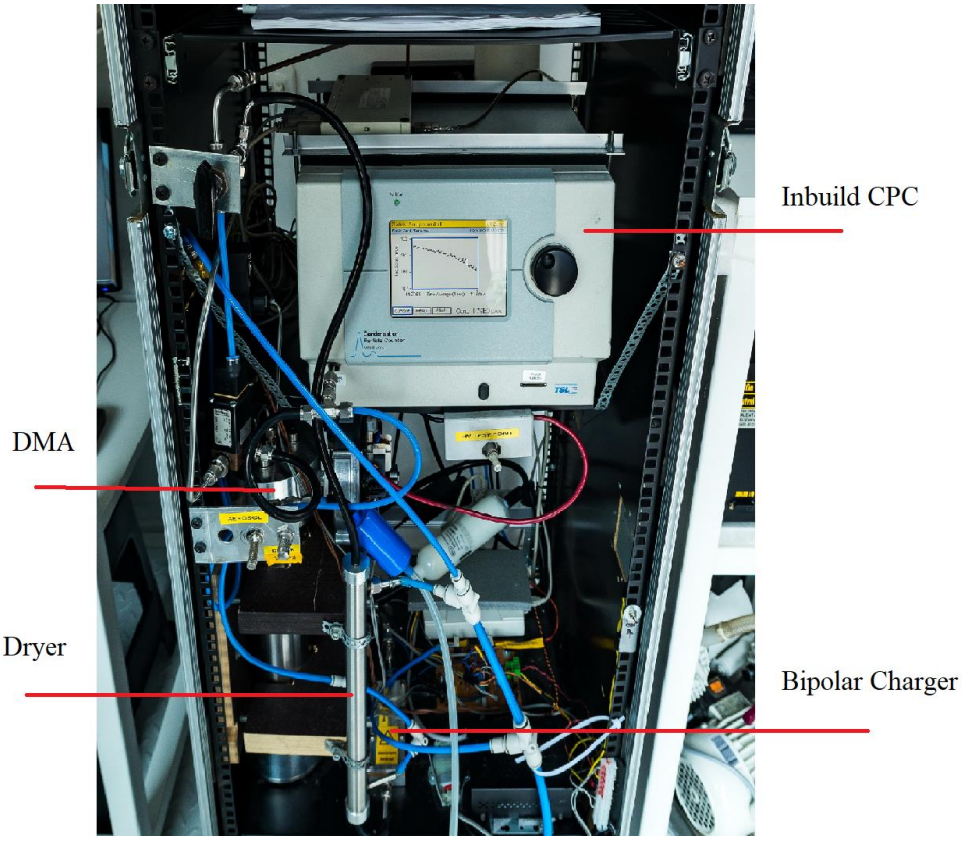

Figure 3: DMPS equipment and its respective components.

3.3.2 Condensation particle counter

The concentration of total *N* (without subdivision in size fractions) was also measured by an independent Condensation Particle Counter (CPC) in 2020 and 2021. The CPC instrument deployed (TSI, model 3752, USA) was operated with an aerosol inlet flow of 1.5 L min^{-1}, and recorded concentrations of particles with a diameter above 4 nm using butanol as a working fluid. Its sampling inlet was made of stainless–steel tube with a diameter of ¼ inch (6.35 mm) and length of ca. 1.6 m. Mean particle number concentrations (N_{CPC}) with a time resolution of 1 second and 1 min were extracted from its extended database.

3.3.3 Meteorological sensors

Meteorological properties were also gathered given the influence of those over the particle concentration and the capability of changing the representativeness of the number of particles generated by the firework. The meteorological data included: Wind Speed (WS), Wind Direction (WD) presented in degrees from North (°) with maximum difference of 180° considering the angle variation for both clockwise and counter–clockwise, Temperature (*T*) and relative humidity (RH).

The meteorological data for air temperature (*T*), relative humidity (RH), wind speed (WS) and wind direction (WD) were obtained on site by standardized methods (HDS2.3 D17, Delta, Italy) with a time resolution of 1 hour in 2009 and 10 minutes for the remaining years.

3.4 Data treatment

Descriptive statistics were made for each aerosol size fraction and meteorological parameter being separated by year and time fraction. Most results considered the mean value with one of the time spans. The central tendency analysis for the aerosol size fraction concentration was different depending on the amount of data points. For larger amount of time like entire day, month or several days, median was chosen as this data presents a log normal distribution. For shorter time periods, like the time between start and end of fireworks, mean was used as with fewer than 30 data points the data presented a normal distribution.

From the measured size distribution, we derived particle number concentrations in the size ranges of 6–100 nm (UF particles) from 100 to 1000 nm (regional or chemically aged particles) and from 6 to 1000 nm (total particles). Contour plots were generated with the size distribution of particles over time. These plots take into consideration the full day time span. On the x-axis of the

plots is the time, on the y-axis is the particle size from 6 to 1000 nm and the concentration is given on color scale from dark blue (lowest) to dark red (highest).

To calculate the respective differences of the aerosol concentrations between the time windows three main methods were used. For comparison of means between different time intervals the *t*-test was the chosen method. By verifying that During-Time had a considerably different variance compared to Before-Time and After-Time, the Welch's *t*-test was used with a confidence interval of 0.90 for the two-tailed test and 0.95 for the one tailed test. The one tailed test assumed the During-Time as having a higher mean than the others.

The second method was the Relative Change (RDiff) which expresses the ratio of the means for the time windows and can be described as:

$$Relative\ Change = \frac{mean(DT) - mean(BT)}{mean(BT)} \quad (1)$$

The difference of means of During-Time (DT) and Before-Time (BT) relative to the mean of the Before-Time. The same was applied to the After-Time (AT).

As the ratios in general are influenced by the magnitude of the parameters a third metric, *z*-value, was derived. The *z*-value can be described as:

$$z - value = \frac{mean(DT) - mean(BT)}{sdev(Whole\ Day)} \quad (2)$$

The mean difference of During-Time (DT) and Before-Time (or After-Time), relative to the standard deviation. The latter property was calculated for the complete day excluding the firework interval (During-Time).

4 Results and discussion

4.1 Identification of firework events at the fixed site

The year 2021 was selected as a starting point to understand the behavior of the fireworks from the aerosol concentrations perspective. This year was selected given its dimension and our capability of being present on the event.

The monitoring of the weather parameters and particle number concentrations for this year extended throughout the entire day. This made it possible to identify any specific time tendency in relation to the rest of the day besides the firework time. Due to the high variability of the WS and WD, their results were averaged by arithmetic mean for 24 minutes. This represents 3 sequential measurements in accordance with DMPS result output frequency. The graphical representation of the daily variation can be seen below on Figure 4 which corresponds to the measurements for 20th of August 2021 where all measurements were matched to an 8-minute time resolution.

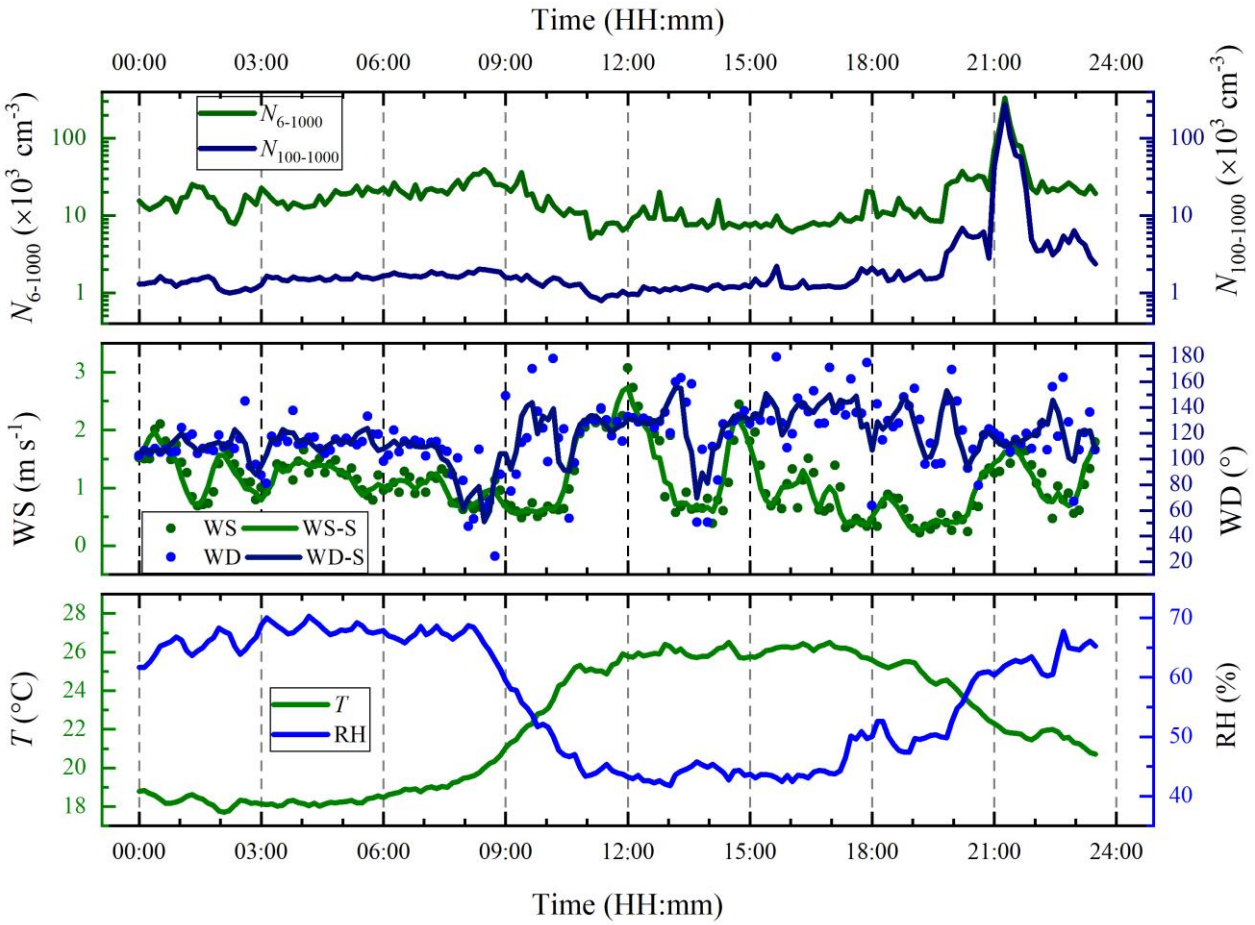

Figure 4: Particle number concentrations ($N_{6–1000}$ and $N_{100–1000}$) and meteorological data (WS, WD, *T* and RH) on 20th of August 2021. The particle concentration was represented in $\log_{10}$ scale for better separation of the measurements.WS-S and WD-S represent the 8-minute smoothed WS and WD data, respectively.

We could observe in 2021 a negative correlation between higher wind speed and the measured aerosol concentration in both fractions. This can be explained by the different particle concentrations in the city and its surroundings. The larger WS brought air masses with lower concentrations into the city. The main aspect was the increase in aerosol concentration after 21:00, with a proportionally stronger increase on the 100–1000 nm size fraction. From the meteorological data it could be observed that the atmospheric conditions were stable and the changes in *N* can be related to their sources and transformation processes.

Due to the sharp increase in aerosol concentration around the firework event time a graphic representation of the total aerosol concentration throughout the entire day with a time resolution of 1 minute was obtained with CPC and is shown on Figure 5.

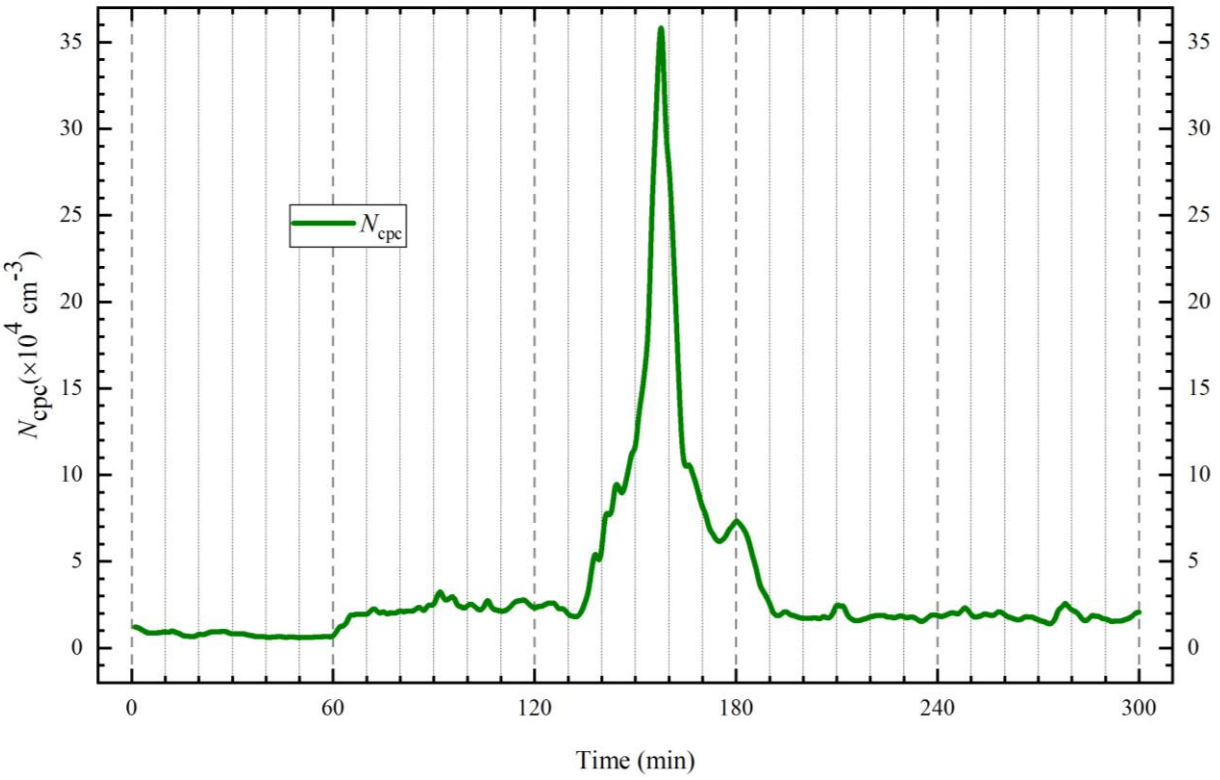

Figure 5: Total particle number concentration (N_{cpc}) over time (in minutes) on 20 of August 2021 from 19:00 to 23:59 with a time resolution of 1 minute.

The CPC measurement gives the visualization of a very sharp rise in aerosol concentration. The central peak lasted for approximately twenty minutes. In 2021 the wind speed was not particularly high (around 1.42 m s^{-1} as mean value). There was a delay of around 15 minutes with respect to the firework spectacle. This comprised a time shift from the beginning to the actual firework activity (at 21:06) and the dispersion of the firework smoke to the measurement site (around 9 to 10 minutes delayed).

From the DMPS and the CPC measurements a max aerosol concentration could be seen above 30 × 10^4 cm^{-3}. This concentration was not measured in Budapest before. Similar concentrations were obtained only in the Castle District Tunnel (Salma et al., 2011b). Such pollution levels happened 5 to 6 minutes after the end of the spectacle, causing a short-term exposure to spectators and people nearby.

4.2 Contour plots

The evolution of the firework effect on the aerosol concentration can be nicely observed also on the contour plots on Figure 6.

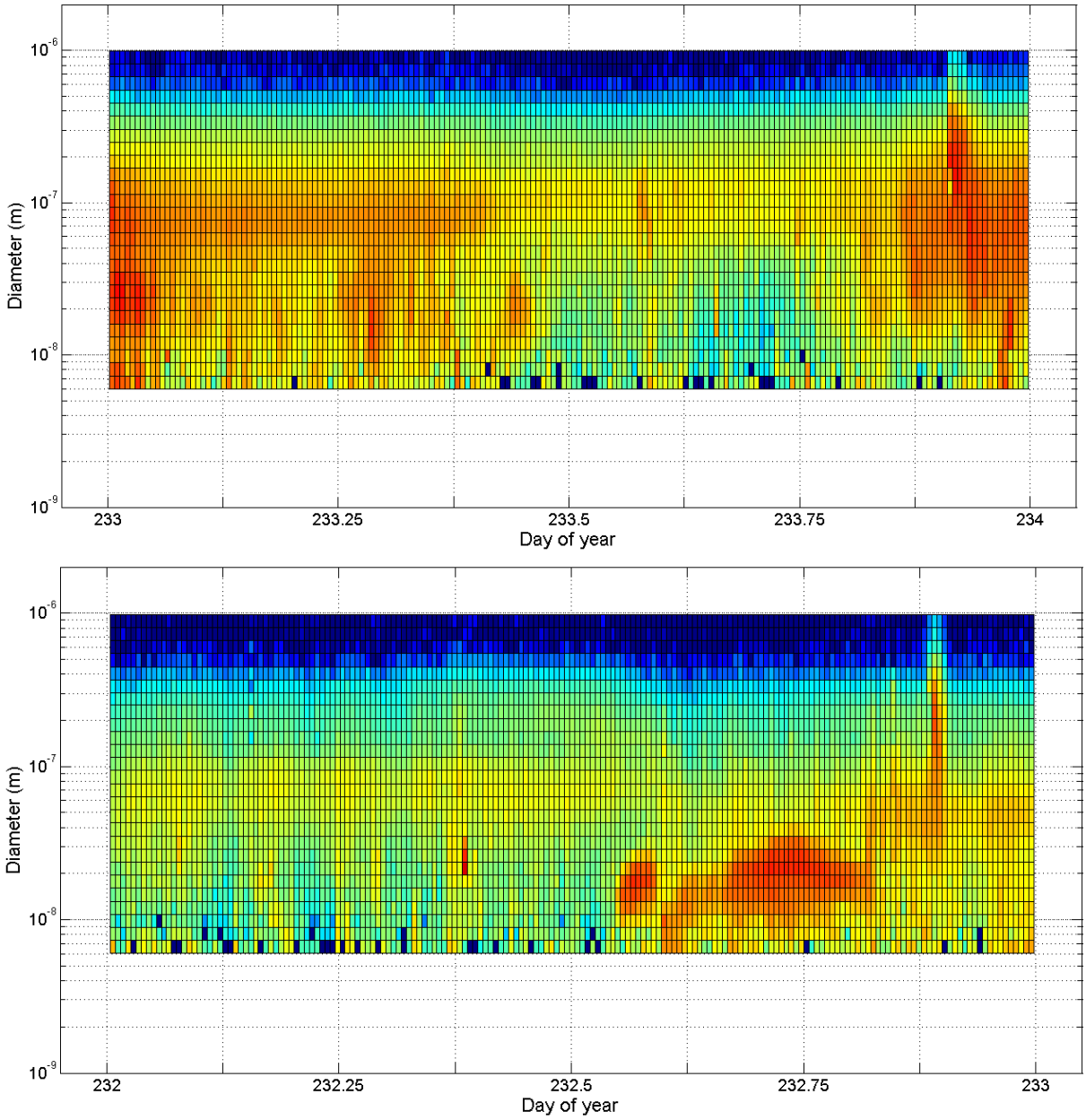

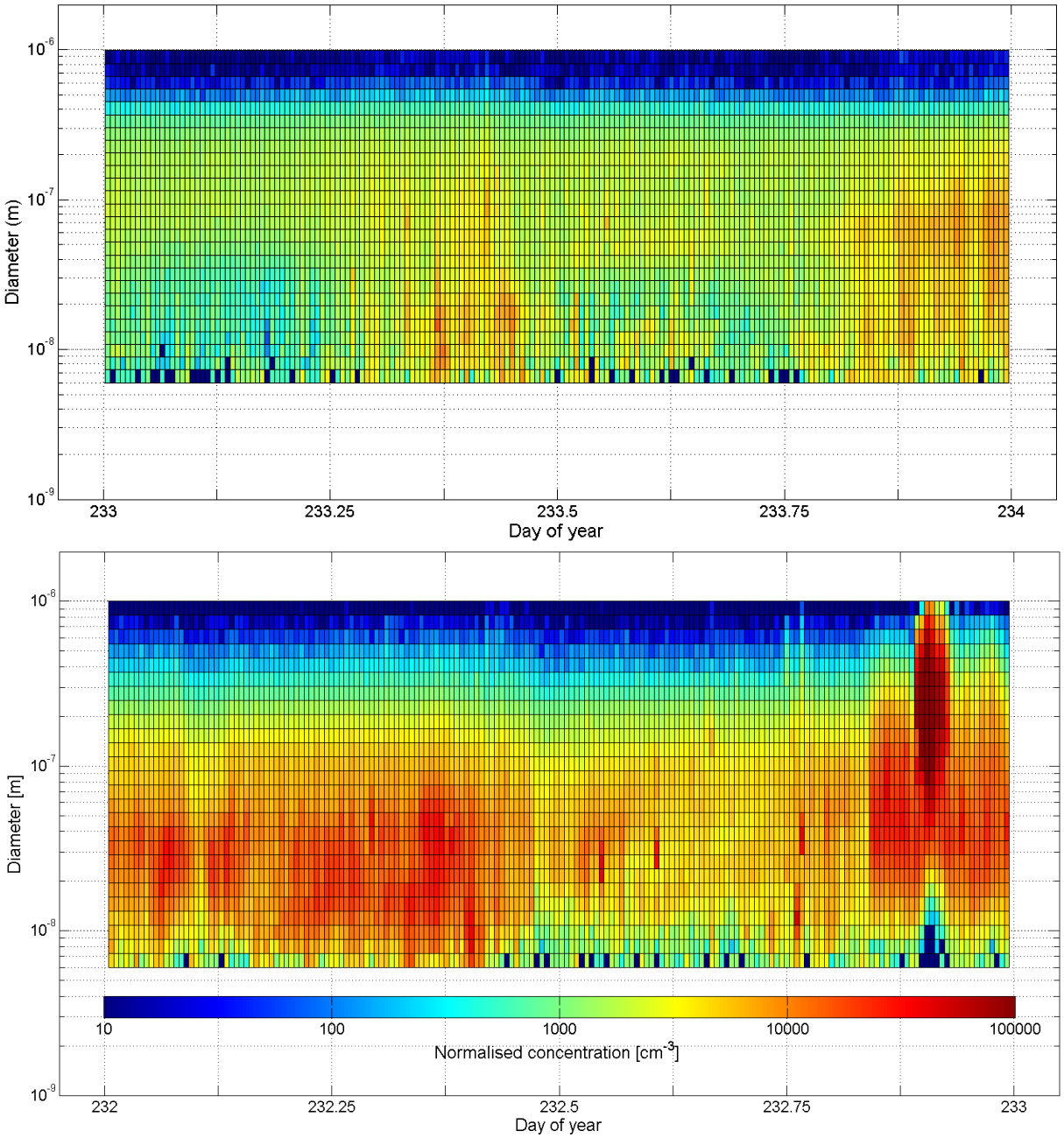

Figure 6: Contour plot of particle number concentrations on 20th of August of (from top to bottom) 2016, 2017, 2020 and 2021.

On all years, it could be seen an overall well distributed pattern of aerosol concentrations until the middle of the day. It was followed by a reduction on the early afternoon and an increase by the beginning of the evening. There was a clear exacerbation for the time corresponding between 21:00 and 22:00 especially in 2021. The exception to this was in 2020. The largest increment happened between 100 and 1000 nm (dark red).

We could also note through the graphical analysis that aerosol concentrations between 20:00 and 21:00 were stable and could be used as comparison parameter (namely the Before-Time). The same could be applied to the time between 22:30 and 23:30 (on this work called After-Time). These findings are in line with the conclusions of the previous section for some years. The actual appearance was different (shorter in 2016), while the three plots were qualitatively similar.

Another aspect pointing out was the higher concentration of aerosols on $N_{100–1000}$ size range than others during or right after the firework events. Further analysis was made by splitting the size fractions to evaluate their behaviors better.

4.3 Ordinary conditions

Daily average values were calculated for all years considered and the results are shown in Table 2. These results were useful to establish a comparison with the guidelines of health authorities regarding maximum values of aerosol concentrations.

Table 2: Daily median values of particle number concentrations (the values are on a 10^{-3} scale) for 20 August of each year.

Year	$N_{6–25}$	$N_{6–100}$	$N_{100–1000}$	$N_{6–1000}$
2009	4.9	10.3	2.0	12.6
2014	2.5	7.0	3.3	10.1
2015	2.9	6.2	1.6	7.8
2016	2.9	7.3	1.9	9.2
2017	1.7	3.6	0.55	4.2
2020	1.6	3.3	1.2	4.6
2021	5.9	13.6	1.5	15.1

The daily median values showed that the levels of UFP concentration did not exceed the limit classified as “High” by the WHO air quality guidelines (2021) of 10×10^3 cm^{-3} in most years besides 2009 and 2021. In any case none of the median values also fit within the category of low concentration. Narrowing down to the Before, During and After time and adding the meteorological conditions the central tendencies changed. The relevant data is summarized in Table 3.

Table 3: Median particle number concentration in the size fractions of 6–100 nm ($N_{6–100}$) and 100–1000 nm ($N_{100–1000}$) both in units of $10^3 cm^{-3}$, mean wind speed (WS in m s^{-1}), wind direction (WD in °), air temperature (T in °C) and relative humidity (RH in %) on 20th August in different years for the time intervals Before-Time (BT), During-Time (DT) and After-Time (AT).

	Parameter	2009	2014	2015	2016	2017	2020	2021
B	$N_{6–100}$	16	8.0	9.2	6.5	6.5	6.1	24
T	$N_{100–1000}$	3.5	2.1	1.7	2.1	0.7	1.4	5.2
	WS	2.0	0.7	3.6	1.4	5.2	0.8	0.5
	WD	130	32	44	166	15	102	120
	T	24	19	19	26	21	25	24
	RH	40	73	61	61	49	52	55
D	$N_{6–100}$	22	11	8.8	12	4.3	7.2	22
T	$N_{100–1000}$	7.6	3.8	2.1	8.2	0.5	1.7	57
	WS	10	0.7	4.4	1.1	4.4	1.2	1.4
	WD	180	30	45	159	9	101	116
	T	22	19	19	25	19	24	22
	RH	46	77	64	65	48	58	62
A	$N_{6–100}$	26	14	6.6	17	6.2	7.1	18
T	$N_{100–1000}$	82	4.6	1.8	3.5	0.7	1.9	4.6
	WS	2	0.9	3.9	0.9	3.7	0.9	0.8
	WD	110	28	44	28	37	143	122
	T	20	18	18	24	18	23	22
	RH	58	83	67	70	53	64	63

From the first analysis we can observe that the aerosol concentrations along the years had a good degree of variability. 2009 and 2021 point out as the years with greatest values during the firework event. Comparing the years with fireworks and the years without (2020) as well as the times before, during and after gives hints of the potential effects of the spectacle on aerosol concentration. It is hard, however, to establish if there is really a considerable difference without more in-depth analysis.

The meteorological parameters values do not point for a simple correlation with aerosol measurements. Although Temperature and Relative Humidity had closer measurements within the same year for the different time frames, the wind speed and direction could change much more abruptly like in 2009 or 2021. The local meteorology, in particular the WD and WS together with the dispersion of the firework smoke determine whether the event can or cannot be detected at a fixed location. These conditions were favorable in 2021, 2017 and 2016 and were preventing the identification in 2014 and 2015.

Referring to the WHO health limits, when observing the measurements closer to firework events, the only years to exceed the 1-h "High" concentration limit of 20×10^3 cm^{-3} (for $N_{6–100}$) were 2021 in Before-Time and During-Time and 2009 in During-Time and After-Time. Considering that those Before-Time include the measurements pre-firework events only and for 2021 their values are even higher than During-Time.

4.4 Particle concentration and ordinary meteorological conditions data distribution

To better understand the behavior of the data of each parameter a measurement of the distribution was calculated. Along with the aerosol concentrations measurements the meteorological parameters were monitored due to the influence they might have had on the results.

The mean values of all years together for the aerosol concentrations and meteorological parameters varied depending on the time span (before, during or after) around the firework events. The three timespans ranged a similar trend as shown in Tables 4, 5 and 6 below. On all those tables "Max" is the maximum average (mean for weather parameters and median for aerosol concentration) value found, "Min" is the minimum average value found, "Central" is the respective central tendency over the years, "% Stdev" is the percent relative sample standard deviation of all years respective to central tendency, and "Max & Min Year" are the years when the respective "Max" and "Min" average values were obtained. As this data took into consideration all years, it presents a large variance in all parameters, but it was useful to understand the span of the measurements of each parameter.

Table 4: Descriptive statistics of the aerosol concentrations and weather parameters for the Before-Time considering all years of measurement. The Central column refers to the central tendency which was median for the aerosol concentrations and mean for the weather parameters. The particle number concentrations are in units of $10^3 cm^{-3}$.

Before–Time	Max	Min	Central	% Stdev	Max & Min Year
$N_{6–100}$	24	6.1	8.0	82	2021 & 2020
$N_{100–1000}$	5.2	0.7	2.1	71	2021 & 2017
WS	5.2	0.5	2.0	86	2017 & 2021
WD	166	15	87	66	2009 & 2014
T	26	19	23	12	2016 & 2015
RH	73	40	56	19	2014 & 2009

On Before-Time we could observe the predominancy of the $N_{6–100}$ fraction compared with the $N_{100–1000}$, yielding a low $N_{100–1000}$/ $N_{6–100}$ ratio. The last had a comparatively smaller standard deviation (standard error). The WS and WD measurements show more changes than the temperature and relative humidity. In any case WS, *T* and RH did not present extreme values.

Table 5: Descriptive statistics of the aerosol concentrations and weather parameters for the During-Time considering all years of measurement. The Central column refers to the central tendency which was median for the aerosol concentrations and mean for the weather parameters. The particle number concentrations are in units of $10^3 cm^{-3}$.

During–Time	Max	Min	Central	%Stdev	Max & Min Year
$N_{6–100}$	22	4.3	11	66	2021 & 2017
$N_{100–1000}$	57	0.5	3.8	529	2021 & 2017
WS	4.4	0.7	2.0	80	2017 & 2014
WD	180	9.4	91	72	2009 & 2015
T	25	19	21	12	2016 & 2014
RH	77	46	60	18	2014 & 2009

The During-Time schedule evidenced an almost inversion of the proportions of the aerosol fractions for Maximum values and an increase for the aerosol median concentrations. There was also a high increase in the variation of the $N_{100–1000}$ fraction. In average $N_{6–100}$ stayed predominant but the proportion of $N_{100–1000}$ increased. Unlike aerosol concentrations, the weather parameters did not change abruptly.

Table 6: Descriptive statistics of the aerosol concentrations and weather parameters for the After-Time considering all years of measurement. The Central column refers to the central tendency which was median for the aerosol concentrations and mean for the weather parameters. The particle number concentrations are in units of $10^3 cm^{-3}$.

After-Time	Max	Min	Avg	% Stdev	Max & Min Year
$N_{6–100}$	26	6.2	14	52	2009 & 2017
$N_{100–1000}$	8.2	0.7	3.5	72	2009 & 2017
WS	3.9	0.8	1.9	74	2015 & 2021
WD	143	28	73	68	2020 & 2015
T	24	18	20	12	2016 & 2017
RH	83	53	65	14	2014 & 2017

On After-Time the particle fractions return to values like the ones found on Before-Time in terms of proportion however, their median values stayed higher. The weather parameters kept the same tendency as shown in Before-Time and During-Time with decrease in temperature, increase in humidity and a high variability for WD and WS.

We could observe that when considering the aerosol concentrations, the highest values were obtained in 2021 During-Time. This was expected due to the dimension of the firework events, the location relative to the measurement site and the time span itself which ranges over the firework event time. In fact, 2021 had the highest aerosol concentrations for the Before-Time and During-Time but not for After-Time, when 2009 had the highest median values. The weather parameter of those years in all three time frames were similar and even with the event in 2021 having much higher proportions than 2009, there are factors that can affect the total aerosol production and atmospheric residence time that could not be monitored.

It was interesting to notice that the lowest values were not found in 2020 (when there were no firework events) but in 2017 After-Time. This might be related to the meteorological conditions and gives a perception on how those parameters can change the results. Also, it is valid to point out that although the fireworks were expected to be the main source of aerosol it was not the only one. The strongest aspect was a confirmation of the initially seen influence of fireworks over $N_{100–100}$ fraction. To understand it better and more refined analysis was done.

4.5 Atmospheric concentrations

A different ratio of increase in concentration was observed for the aerosol in particle size 6–100 nm ($N_{6–100}$) compared to particle size 100–1000 nm ($N_{100–1000}$). The percentage proportion of $N_{100–1000}$ in relation to the total particle size 6–1000 nm ($N_{6–1000}$) can be seen on Table 7 where each year ratio is given and the respective percentage difference between Before-Time ratio and During-Time and After-Time.

Table 7: Ratio of particle number concentrations for the fraction of 100–1000 nm size fraction in relation to total particles ($N_{100–1000}/N_{6–1000}$). The calculation of the ratio was considered as the sum of all results for each time range (Before-Time, During-Time, After-Time) for $N_{100–1000}$ divided by the sum of the respective time range of $N_{6–1000}$. % Diff DB is the percentage difference between During–Time ratio in relation to Before–Time ratio. % Diff DA is the percentage difference between During–Time ratio in relation to After–Time ratio. All values are in percentage (%).

Years	Before–Time	During–Time	After–Time	% Diff DA	% Diff DB
2009	18	26	24	43	8.4
2014	21	26	24	24	8.3
2015	16	20	22	23	–10
2016	24	40	17	64	130
2017	10	11	9.5	7.5	14
2020	19	19	21	3.3	–8.4
2021	18	72	20	297	250

On the years with firework events there was a higher proportion of particle 100–1000 nm ($N_{100–1000}$) on During-Time. The exception was 2015 when the After-Time had the highest proportion. The years 2014 and 2015 had a smaller variation on the ratio, comparable to the year reference for no fireworks (2020). We can also observe that in the years with a proportionally higher increase in overall aerosol particles there were also higher $N_{100–1000}/N_{6–1000}$ ratios. In 2017 although the time range and ratio pattern can be also observed the total concentrations are significantly lower. This difference could be partially attributed to the WS being higher this year and a similar effect can be seen also in 2015. The highest ratio of $N_{100–1000}/N_{6–1000}$ was observed in 2021 on During-Time. The Before and During-Time had comparable rages to the other years.

4.6 Size distributions.

Particle number size distribution for Before, During and After the firework activity in 2021 are shown in Figure 7:

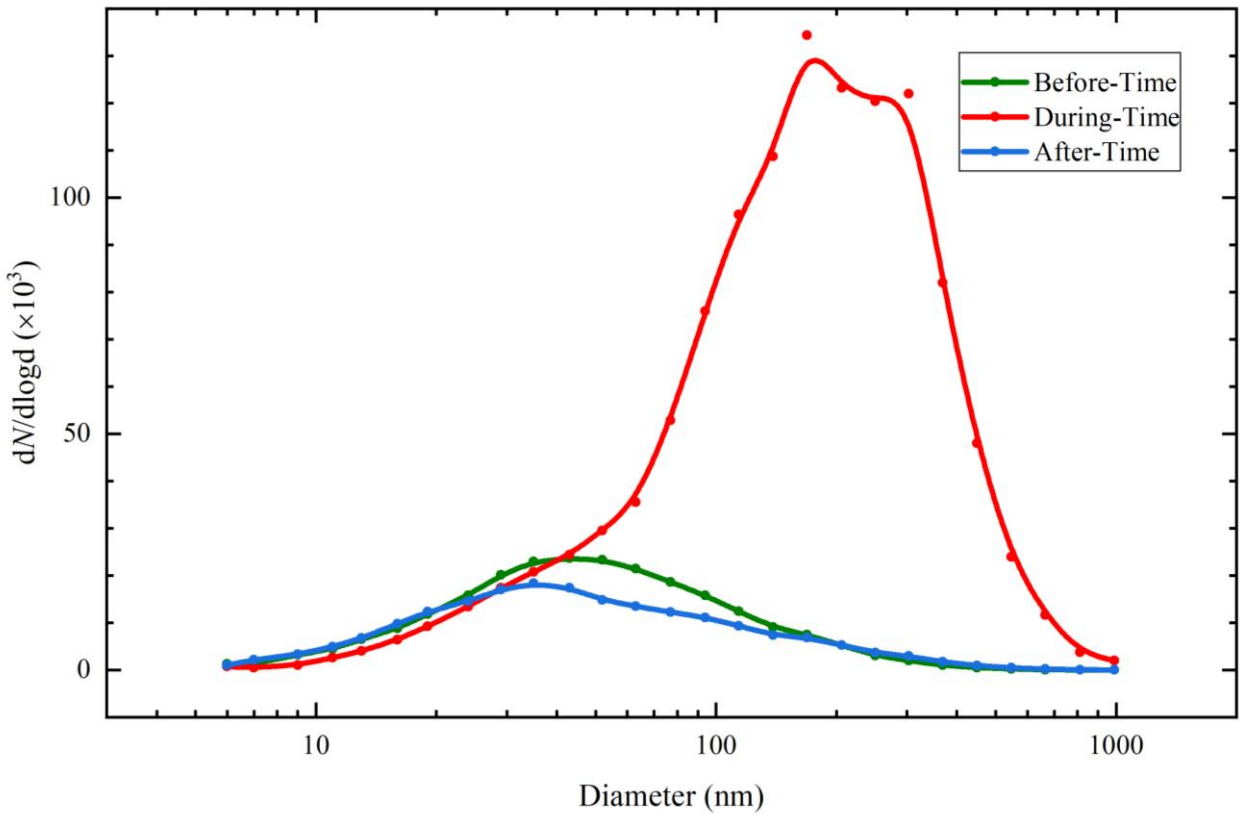

Figure 7: Particle size distribution for Before-Time (20:00 - 21:00), During-Time (21:00 - 22:00) and After-Time (22:30 - 23:30) in 2021.

The particle size distribution was similar between Before-Time and After-Time while During-Time stands with a visible higher particle counts between 50 and 600 nm. The peak of distribution for During-Time is between 100 and 400 nm. This is larger than any previously observed modal diameter in Budapest. For the Before and After-Time there is a slight difference in the shape of the curves. The local maxima and minima follow the same pattern, with some difference that would be expected given the 1.5 hour of difference between the end of one and beginning of the other. The unusually large diameter observed in During-Time contradicts the high deflagration temperature (up to 2500 °C).

The peak shift to the right in the During-Time didn't strongly affect the aerosol particles concentration between 6 and 30 nm and that portion of the curve is quite similar to the other two time-ranges. A large amount of aerosol particles of larger sizes was produced.

Other studies have shown similar trends of increase in the accumulation mode of aerosol together with firework events. In some cases, the increase in particle size was slightly shifted to smaller particles as for the Diwali observations (Yadav et al., 2019) where it was suggested that the initial burst increase the nucleation mode concentrations, where ultrafine particles would be generated, followed by a shift with time from Aitken mode to Accumulation mode.

Along the seven years analyzed the results followed a trend in reference to the size distribution which could be given as years 2020 and 2021, being respectively the years of most and least even distribution in particle size. Focusing more specifically on the During-Time, a selection of the particle size ranges with the highest proportional abundance from the median value was made: in 2009 the proportional highest contributions of particles (making 52% of total) were between 42 and 94 nm. in 2014 (making 51%) were between 29 and 94 nm. In 2015 (making 53%) were between 19 and 94 nm. In 2016 (making 56%) were between 43 and 170 nm. In 2017 (making 53%) were between 28 and 139 nm. In 2020 (making 54%) were between 16 and 77 nm. In 2021 (making 52%) were between 138 and 307 nm. A representation of the integral size distributions can be seen on Figure 8.

Considering the extremes, a similar tendency was found by Li et al., 2019 were during fireworks the size range the major proportions were 100–180 nm (30%), 180–320 nm (25%), and 56–100 nm (20%) and during non– firework events the major proportions were of 56–100 nm (28%), 100–180 nm (20%), and 32–56 nm (19%). Their results are more compatible with the years 2016 and 2017 of our measurements.

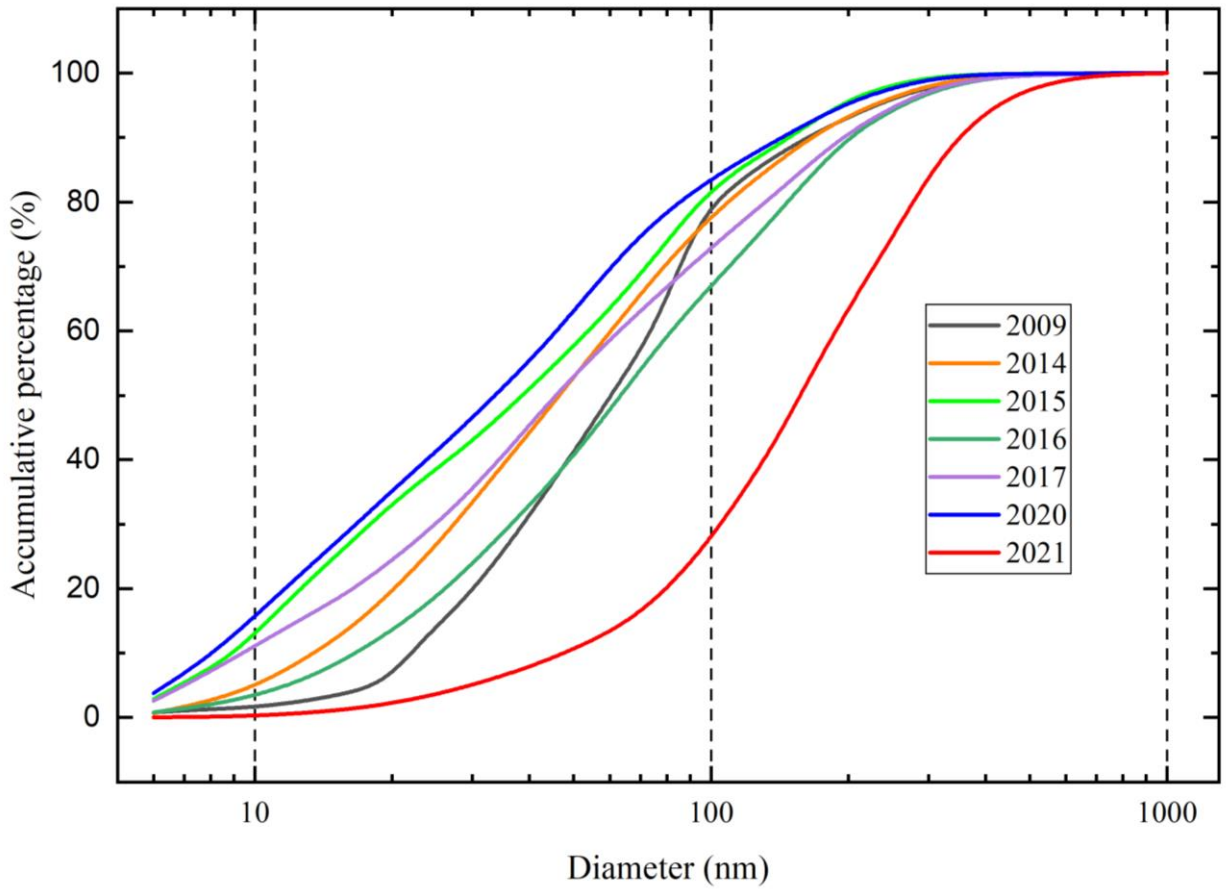

Figure 8: Integral distribution of particle number concentrations for each year.

As described by the numbers, the graphical representation has shown the shift to the right (to higher values of) in relation to particle diameter for the years with aerosol concentration. The strongest aspect is how the Accumulative mode slope becomes bigger and more centered between 80 and 300 nm particle diameter when the firework-proportional-increase in aerosol concentration is detected. The two extremes of no firework events (2020) and highest intensity firework events (2021) form a clear border and within it are the curves for the other years.

4.6.1 Changes in various size fractions

To look for more details on the question if the increase in the Accumulation mode could be related to an initial increase in the Aitken mode as suggested in other studies, time series of the concentrations in distinct size fractions were prepared and are shown in graphical mode in Figure 9 for years 2009, 2014 and 2015 and Figure10 for years 2016, 2017, 2020 and 2021.

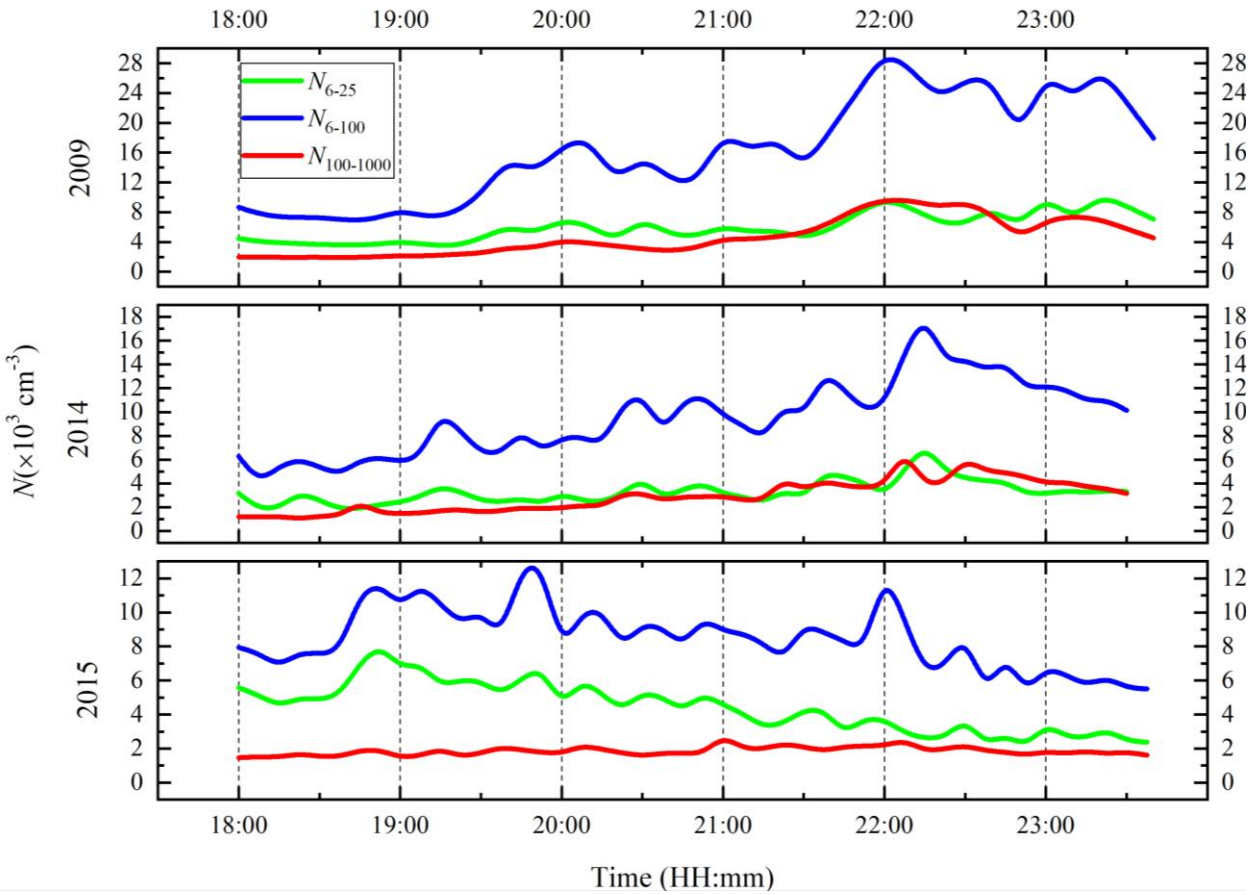

Figure 9: Time series of particle number concentration in diameter ranged of 6–25 nm ($N_{6–25}$), 6–100 nm ($N_{6–100}$) and 100–1000 nm ($N_{100–1000}$) on 20th of August from 18:00 to 23:59 in the years 2009, 2014 and 2015.

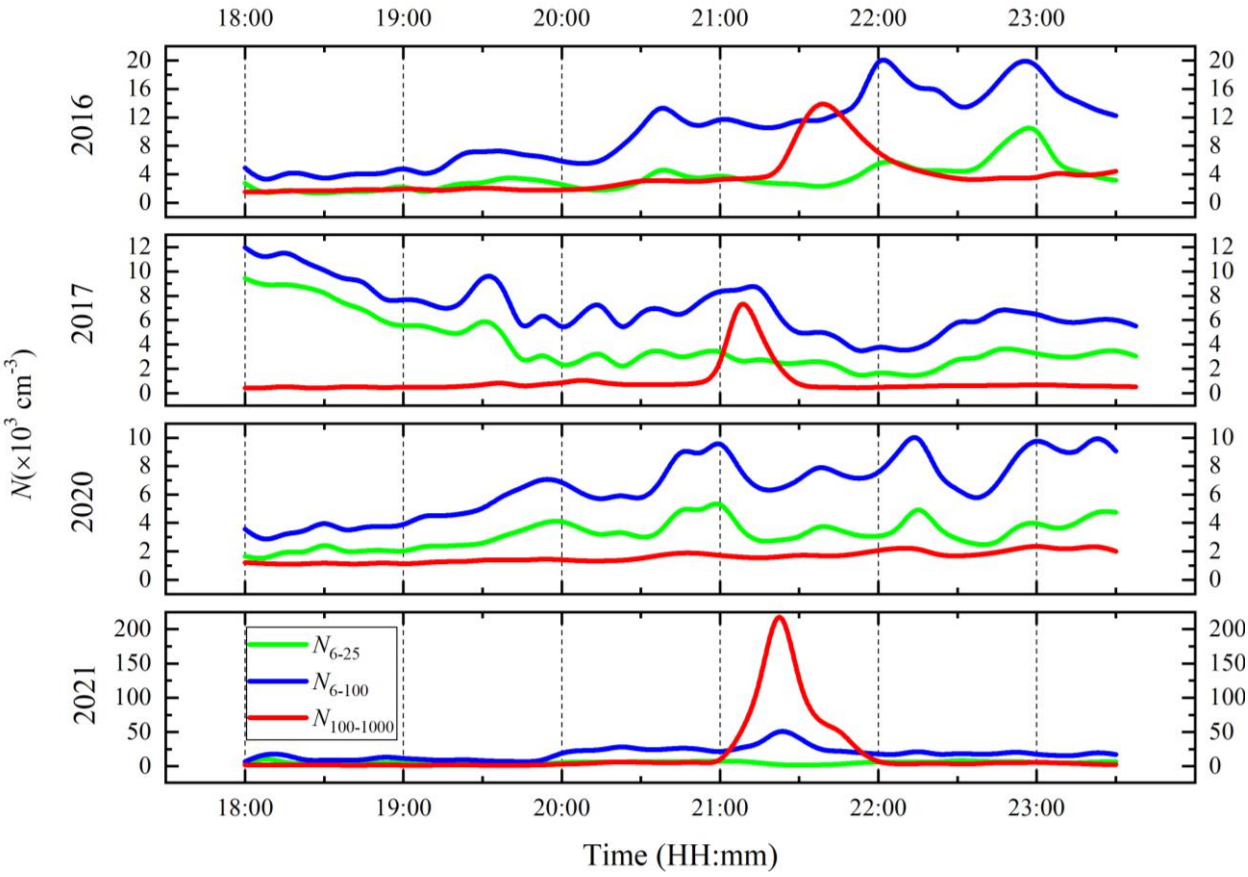

Figure 10: Time series of particle number concentration in diameter ranged of 6–25 nm ($N_{6–25}$), 6–100 nm ($N_{6–100}$) and 100–1000 nm ($N_{100–1000}$) on 20th of August from 18:00 to 23:59 in the years 2016, 2017, 2020 and 2021.

The change from Aitken mode to Accumulation mode is not observable or not clear on the visual representations. In most years, considering that the fireworks always start at few minutes after 21:00, it is more visible that the Accumulation mode corresponding to particle 100–1000 nm ($N_{100–1000}$) concentrations start increasing before the ones in the Aitken, especially when we compare the smaller fractions corresponding to particle size between 6–25 nm ($N_{6–25}$). In any case it is important to point out that one of the other studies that found this correlation the firework events were more scattered in area and the aerosol concentration average was considered for longer time ranges. $N_{100–1000}$ indicates to be the most sensitive to firework activity. $N_{6–25}$ and $N_{6–100}$ are not suitable for this purpose in line with the conclusions and results from size distributions.

The relatively large diameters are unusual when considering the elevated temperatures up to 2500 °C accompanying the pyrotechnic deflagration. The explosions take place, however, in a dispersed manner which is far from steady-state volumetric combustion conditions, and this results

in considerable *T* gradients and turbulent air flows. Most particles were likely generated in adjacent zones with lower temperatures, which could explain the larger diameters. The particle sizes can also be influenced by changes in the equivalent diameters of the freshly emitted particles which are transformed from chain-like morphology to more compact structures (Cao et al., 2018). The hygroscopic diameter growth of fresh firework particles at larger RHs – for instance above the river – can also make the smoke thicker. The dense smoke of these particles is well visible in the fading out lights of explosion and can even degrade the visibility in extended air spaces. This is known to providers of organized fireworks, and it also contributes to the fact that planned pauses are scheduled regularly during the show.

4.7 Characteristics of firework events versus non-event intervals

From the general analysis the proper time limits for Before, During and After-Time could be well defined and the size fraction $N_{100–1000}$ was verified as of higher importance for understanding the firework aerosol phenomenon. With these assumptions the proportion comparisons between event and non-event time were performed considering the high variability of the data. The whole size fraction $N_{6–1000}$ was also included as the second most affected by the fireworks. The relative change was calculated for the Before-Time with During-Time. The same was done between After-Time and During-Time. The results can be seen on table 8.

Table 8: Mean aerosol concentration comparison (RDiff) for each year and each size category. BD stands for Before-Time and During-Time scores, AD stands for After-Time and During-Time scores.

Years - RDiff	BD $N_{100–1000}$	BD $N_{6–1000}$	AD $N_{100–1000}$	AD $N_{6–1000}$
2009	0.4	0.1	-0.4	-0.3
2014	0.3	0.2	-0.3	-0.3
2015	0.2	0.0	0.1	0.3
2016	1.4	0.6	0.6	-0.2
2017	2.0	0.3	2.8	0.4
2020	0.2	0.3	-0.1	0.0
2021	18	3.4	18	4.1

We could observe here a clear tendency of increase in the aerosol concentration on During-Time compared to the Before-Time. For the years 2014 and 2015 the increase was rather small and even comparable with the same results for the year 2020 when there was no firework event. On

2016, 2017 and exceptionally 2021 there was a significant raise in the values especially for $N_{100–1000}$ fraction. The level of increase for 2021 was still quite above the one found by Lin et al., 2016, where the $N_{100–1000}$ fraction was 14 times higher versus 18 times for our 2021 data when they also compared firework non-events with firework events. The negative values observed on the During After-Time comparison indicate that the After-Time had higher concentrations than the During-Time. Nonetheless from 2015 to 2021 the Before During and During After-Time comparisons ranged comparable results. Further the *z*-value, relative to the daily standard deviation, was also calculated as shown on Table 9.

Table 9: *Z*-value. BD stands for the *z*-value between Before-Time and During-Time, AD stands for *z*-value between After-Time and During-Time.

Years - *z*-value	BD $N_{100–1000}$	BD $N_{6–1000}$	AD $N_{100–1000}$	AD $N_{6–1000}$
2009	0.7	0.4	-1.8	-1.6
2014	0.7	0.7	-1.3	-1.5
2015	1.2	-0.1	1.0	0.7
2016	2.6	1.1	1.6	-0.5
2017	10	0.7	11	0.8
2020	0.9	0.8	-0.9	-0.1
2021	18	9.9	18	10

The tendencies from RDiff calculation were repeated in *z*-value with a strengthening of the difference scores. Interesting to notice that 2021 had no difference on $N_{100–1000}$ and an increase for $N_{6–1000.}$ The aerosol concentration means of the During-Time tended to be greater than the Before-Time. The same did not hold true when comparing During and After-Time. For $N_{100–1000}$ 2009, 2014 and 2020 the After-Time means were higher than During-Time specially for the first two years. Similarly, for $N_{6–1000}$ the same happened on 2009, 2014, 2016 and 2020. It was again very characteristic to see the fraction $N_{100–1000}$ with the highest scores. For comparing the averages and assuming the times have different population variances a Welch's two-tailed *t*-test results was performed, and the results are available on Table 10.

Table 10: Welch's two-sided *t*-test for means comparing data from During-Time to Before-Time (BD) and During-Time to After-Time (AD) both for $N_{100–1000}$ and $N_{6–1000}$. The results are the respective *p*-values.

Year - Welch's Two Sided	BD $N_{100–1000}$	BD $N_{6–1000}$	AD $N_{100–1000}$	AD $N_{6–1000}$
2009	0.04	0.26	0.01	0.00
2014	0.03	0.06	0.00	0.00
2015	0.08	0.57	0.13	0.00
2016	0.07	0.01	0.23	0.13
2017	0.17	0.22	0.14	0.16
2020	0.00	0.01	0.06	0.83
2021	0.06	0.06	0.06	0.05

Through the two-sided Welch's *t*-test a 0.9 confidence was considered. Significantly different means were observed in the Before-During comparison, for $N_{100–1000}$ in all years except 2017 and for $N_{6–1000}$ fraction in 2014, 2016, 2020 and 2021. Also, significantly different means were observed in the After-During, for $N_{100–1000}$ fraction in 2009, 2014, 2020 and 2021 and for $N_{6–1000}$ fraction in 2009, 2014, 2015 and 2021. A one-sided Welch's test was done considering that the During-Time mean would be higher than the others. The results are in Table 11.

Table 11: Welch's one-sided t–test for means of data from During-Time to Before-Time (BD) and During-Time to After-Time (AD) both for $N_{100–1000}$ and $N_{6–1000}$. Results showing the respective *p*-values.

Year - Welch's One Sided	BD $N_{100–1000}$	BD $N_{6–1000}$	AD $N_{100–1000}$	AD $N_{6–1000}$
2009	0.02	0.13	0.99	1.00
2014	0.01	0.03	1.00	1.00
2015	0.04	0.71	0.07	0.00
2016	0.04	0.01	0.12	0.94
2017	0.09	0.11	0.07	0.08
2020	0.00	0.01	0.97	0.59
2021	0.03	0.03	0.03	0.03

Through the one-sided Welch's *t*-test and considering a 0.95 confidence interval there was a distinct set of results for During-After. In the Before-During in both fractions the scores changed but the same tendency was kept. In the After-During comparison, for $N_{100–1000}$ fraction only 2021 and for $N_{6–1000}$ 2015 and 2021 had significantly different means.

Given that the *t*-test has shown a small difference on the *p*-values in 2020 and 2021 it was necessary to use more fine-grained data for the same test. Such data was available only for the total concentration ($N_{6–1000}$) through the CPC measurements. Considering the same time schedules, the data was collected into 3 different time intervals: every 1 second (1s), 30 seconds (30s) and 1 minute (1min). The results of this Welch's t-test are in table 12.

Table 12: Welch's two and one-sided *t*-test for means of data from During-Time to Before-Time (BD) and During-Time to After-Time (AD) for $N_{6–1000}$. Results showing the respective *p*-values.

Time Frequency	Years	Two-Sided BD	Two-Sided AD	One-Sided BD	One-Sided AD
1s	2020	0.0	1.3×10^{-08}	0.0	6.4×10^{-09}
	2021	0.0	0.0	0.0	0.0
30s	2020	1.7×10^{-13}	0.26	8.4×10^{-14}	0.13
	2021	5.1×10^{-17}	2.3×10^{-18}	2.6×10^{-17}	1.1×10^{-18}
1min	2020	2.3×10^{-08}	0.38	1.1×10^{-08}	0.19
	2021	4.1×10^{-09}	9.2×10^{-10}	2.0×10^{-09}	4.6×10^{-10}

The *p*-values have been reduced with the increase of data points for the same time range for both Before-During and During-After comparisons. In any case 2021 has shown *p*-values several orders of magnitude smaller than 2020. The results for 2020 showed a tendency of higher values for the During-After comparisons while 2021 did not.

For 1 second frequency the *p*-values are extremely low (rounded to 0) in 2020 Before-During and low for After-During comparisons. Zero *p*-values in 2021 were found in the Before-During and During-After comparison, leading to the conclusion that on both years and tests the Before and During means are significantly different. The 2020 During-After comparison is much higher than the Before-During but with a 0.9 and 0.95 confidence interval for two-sided and one-sided test respectively it would also be considered that the During-After means are significantly different.

For the 30 second frequency the *p*-values are higher than 1 second frequency. On both years and test types, the *p*-value indicates that the means of Before and During are significantly different, with 2021 scores being much lower than 2020 scores. On the During-After comparison 2021 *p*-values still indicate a significant difference of means. In 2020 they are higher and from the intervals

for one-sided and two-sided tests there would be no difference between the means. The same is applicable on the 1-minute frequency even if the *p*-values had an overall increase.

This phenomenon can have been influenced by the natural decrease in aerosol concentrations after twilight. From 20:00 to 23:59 it would be natural to observe a reduction in the background particle concentrations due to the reduction of their sources. If the concentrations in Before-Time are naturally higher compared to the During-Time, the fireworks produced aerosols would have to compensate and surpass this difference to yield a significantly different mean. The same factor has the opposite effect on the During-After comparison as the During time would be naturally higher than the after time and with fireworks aerosols on During-Time this difference of means would be even higher. The fluctuations on the concentrations along the time detected on the previous analyses seem to surpass this effect, quite visibly in 2020.

It is important to consider that these results refer to the total particle concentrations and therefore are not specifically targeted to the $N_{100–1000}$ fraction whereas our previous results indicate there was the highest changes in concentration. Nonetheless, there was a clear difference between 2020 and 2021 and the fireworks seems have significantly changed the During-Time concentrations compared to the natural background difference.

5 Conclusion

The traditional firework spectacle in Budapest on the 20th of August has the capability of generating a significant amount of aerosol particles which are mostly concentrated within a limited space and time. The particles produced were majorly concentrated in the 100–1000 nm range and the more intense the firework event was the higher the participation of this fraction on the total aerosol particle count concentration. Considering the behavior, fireworks seem to yield a characteristic proportion of size distribution which is differentiable from the usual urban background air pollution. In 2021, when the biggest event from our timeseries was held, the level of aerosol production reached points which could be considered harmful for human health and this factor should be considered when planning such events. The $N_{100–1000}$ was raised in a 1 hour average up to 18 times the background levels and the total particles concentration reached 1-minute maximum mean levels of 369×10^3 cm^{-3}.

As happens for many phenomena in aerosol chemistry the data generated by the aerosols from fireworks have a high variability. This wide range and constant change of values has proven a challenge when comparing event and non-event times. The statistical tests designed in this work to evaluate the level of difference have shown signs of influence of the fireworks on the aerosol concentrations. Nonetheless, the natural variability of those values limited our capability to discern at which degree the fireworks influence on the measurements.

To better understand fireworks from the aerosol and atmospheric perspective it would be interesting to add other methods to collect information. As demonstrated from the statistical analysis there is an influence of several other factors, among them the meteorological conditions. Creating a meteorological model that can include the weather parameters, geography and data about the event and region activity could probably lead to a better differentiation of data coming from time during fireworks compared to neighboring times.

Determination of the atmospheric concentrations of firework-related hazardous aerosol substances is limited by the time resolution of classical sampling devices and by the smallest sample amounts needed for chemical analyses. Online aerosol measuring systems such as high-resolution time-of-flight aerosol mass spectrometers (HR-ToF-AMS) can overcome these obstacles (Drewnick et al., 2006; Jiang et al., 2015; Zhang et al., 2019). Particle number concentrations and size distributions can be also determined with high time resolution (Wehner et al., 2000;

Mönkkönen et al., 2004; Zhang et al., 2010). Moreover, the relatively short atmospheric residence time of the submicrometer particles is beneficial for investigating their sources and transformation processes. Particle mass can be assessed from particle number size distribution, whereas the chemical composition can be estimated from parallel or auxiliary experiments. Most measurement results were obtained in Asia (mainly in China and India), and the data from Europe are sparse (Cao et al., 2018).

Another tool that can be interesting is the use of drones to capture data from closer and have a better understanding of the special distribution of the fireworks. As these types of events are not uniform with diverse types of effects happening at various places and time, the data recorded by the drones could add more details to the model suggested. Also having low-cost sensors that can be spread over a larger area would increase the spaciotemporal resolution.

This work focused on the particle count size ranges. However, it would be a useful addition to also collect the aerosol chemical composition specially in what is tangent to the metals utilized on firework manufacturing. This data would allow the identification of the particles produced that are more likely related to the fireworks rather than on other sources given that the latter very rarely contain compounds such as Sr or Mn. If this compound could be done on distinct size fractions, it would probably give an even better understanding on the size distribution of aerosols produced exclusively by fireworks.

6 References

Ambade B., and Ghosh S. (2013). Characterization of PM10 in the ambient air during Deepawali festival of Rajnandgaon District, India. Natural Hazards, 69, 589-598.

Attri A.K., Kumar U., Jain V.K., (2001). Formation of ozone by fireworks. Nature 411, 1015.

Baranyai E., Simon E., Braun M., Tóthmérész B., Posta J., Fábián I. (2015). The effect of a fireworks event on the amount and elemental concentration of deposited dust collected in the city of Debrecen, Hungary. Air Quality, Atmosphere and Health 8, 359-365.

Berend L. N., Szakács J., Zsolt B. (2007). "The kingdom of Hungary". In Berend, Nora (ed.). Christianization and the Rise of Christian Monarchy: Scandinavia, Central Europe and Rus', c. 900–1200. Cambridge University Press, 319–368.

Cao X., Zhang X., Tong D. Q., Chen W., Zhang S., Zhao H., Xiu A. (2018). Review on physicochemical properties of pollutants released from fireworks: environmental and health effects and prevention. Environmental Reviews, 26, 133-155.

Cartledge B., (2011). The Will to Survive: A History of Hungary. C. Hurst & Co., 14.

Curtis L., Rea W., Smith-Willis P., Fenyves E., Pan Y. (2006). Adverse health effects of outdoor air pollutants. Environment International, 32, 815-830.

Drewnick F., Hings S.S., Cutius J., Eerdekens G., Williams J., (2006). Measurement of fine particulate matter and gas–phase species during the new year's fireworks 2005 in Mainz, Germany. Atmospheric Environment, 40, 4316–4327.

Dyer Ball J., Things Chinese (Kelly and Walsh, Ltd., Shanghai, 1925).

Fleischer O., Wichmann H., Lorenz W., (1999). Release of polychlorinated dibenzo–p–dioxins and dibenzofurans by setting off fireworks. Chemosphere, 39, 925–932.

Gernet J., (1962). Daily Life in China on the Eve of the Mongol Invasion, 1250–1276. Translated by H.M. Wright. Stanford: Stanford University Press, 186.

Gonzalez I.V.R., Reyna–Velarde R., Guerrero–Barajas C., Gonzalez V.S.R., Ordaz A., (2017). Massive burning of fireworks: a pollutant show. Revista Biociencias, 4.

Griffiths T. T., Krone U., Lancaster R., (2017). "Pyrotechnics". Ullmann's Encyclopedia of Industrial Chemistry, Weinheim: Wiley–VCH.

Gouder C., and Montefort S. 2014. Potential impact of fireworks on respiratory health. Lung India: Official Organ of Indian Chest Society, 31, 375-379.

Hickey C., Gordon C., Galdanes K., Blaustein M., Horton L., Chillrud S., Gordon T. (2020). Toxicity of particles emitted by fireworks. Particle and fiber toxicology, 17, 1-11.

Jiang Q., Sun Y. L., Wang Z., Yin Y. (2015). Aerosol composition and sources during the Chinese Spring Festival: fireworks, secondary aerosol, and holiday effects. Atmospheric Chemistry and Physics, 15, 6023-6034.

Jing H., Li Y. F., Zhao J., Li B., Sun J., Chen R., Chen C., (2014). Wide–range particle characterization and elemental concentration in Beijing aerosol during the 2013 Spring Festival. Environmental Pollution, 192, 204–211.

Joshi M., Khan A., Anand S., Sapra B. K., (2016). Size evolution of ultrafine particles: Differential signatures of normal and episodic events. Environmental Pollution, 208, 354–360.

Kató M., Kató A,, Daily News Hungary, https://dailynewshungary.com/, Fiery Budapest: the 20 August Fireworks. (19–August –2014).

Kató M., Kató A., Daily News Hungary, https://dailynewshungary.com/, August 20 programs. (18–August 2015).

Kató M., Kató A., Daily News Hungary, https://dailynewshungary.com/, Hungary's National Holiday – 20 August 2016. (16–August–2016).

Kató M., Kató A., Daily News Hungary, https://dailynewshungary.com/, Fireworks of 20 August to change style and place in Budapest. (03–August–2017).

Kulshrestha U.C., Nageswara Rao T., Azhaguvel S., Kulshrestha M.J., (2004). Emissions and accumulation of metals in the atmosphere due to crackers and sparkles during Diwali festival in India. Atmospheric Environment, 38, 4421–4425.

Lai Y.H., Brimblecombe P., (2017). Regulatory effects on particulate pollution in the early hours of Chinese New Year, 2015. Environmental Monitoring and Assessment, 189, 467.

Lin C.C., Yang, L.S., Cheng Y.H., (2016). Ambient PM2.5, Black Carbon, and Particle Size–Resolved Number Concentrations and the Ångström Exponent Value of Aerosols during the Firework Display at the Lantern Festival in Southern Taiwan. Aerosol and Air Quality Research, 16, 373–387.

Liu D.Y., Rutherford D., Kinsey M., Prather K.A., (1997). Realtime monitoring of pyrotechnically derived aerosol particles in the troposphere. Analytical Chemistry, 69, 1808–1814.

Mönkkönen P., Koponen I.K., Lehtinen K.E.J., Uma R., Srinivasan D., Hämeri K., Kulmala M., (2004). Death of nucleation and Aitken mode particles: observations at extreme atmospheric conditions and their theoretical explanation. Journal of Aerosol Science, 35, 781–787.

Moreno T., Querol S., Alastuey A., Minguillon M.C., Pey J., Rodriguez S., Miro J.V., Felis C., Gibbons W., (2007). Recreational atmospheric pollution episodes: inhalable metalliferous particles from firework displays. Atmospheric Environment, 41, 913–922.

Moreno T., Querol X., Alastuey A., Amato F., Pey J., Pandolfi M., Kuenzli N., Bouso L., Rivera M., Gibbons W., (2010). Effect of fireworks events on urban background trace metal aerosol concentrations: is the cocktail worth the show? Journal of Hazardous Materials, 183, 945–949.

Pearson P., Britton J., McKeever T., Lewis SA., Weiss S., Pavord I., Fogarty A., (2005). Lung function and blood levels of copper, selenium, vitamin C and vitamin E in the general population. European Journal of Clinical Nutrition, 59,1043.

Perry K.D., (1999). Effects of outdoor pyrotechnic displays on the regional air quality of Western Washington State. Journal of Air & Waste Management Association, 49,146–155.

Peshin S.K., Sinha P., Bisht A., (2017). Impact of Diwali firework emissions on air quality of New Delhi, India during 2013–2015. Mausam, 68, 111–118.

Pope R.J., Marshall A.M., O'Kane B.O., (2016). Observing UK Bonfire Night pollution from space: analysis of atmospheric aerosol. Weather, 71, 288–291.

Ravindra K., Mittal A.K., Van Grieken R., (2001). Health risk assessment of urban suspended particulate matter with special reference to polycyclic aromatic hydrocarbons: a review. Reviews on Environmental Health, 16, 169–189.

Russell M. S., (2009), The chemistry of fireworks. Royal Society of Chemistry.

Salma I., Borsós T., Weidinger T., Aalto P., Hussein T., Dal Maso M., Kulmala M., (2011a). Production, growth and properties of ultrafine atmospheric aerosol particles in an urban environment, Atmospheric Chemistry and Physics, 11, 1339–1353.

Salma I., Borsós T., Aalto P., Kulmala M., (2011b). Time-resolved number concentrations and size distribution of aerosol particles in an urban road tunnel, Boreal Environment Research, 16, 262–272.

Salma I., Németh Z., Kerminen V.–M., Aalto P., Nieminen T., Weidinger T., Molnár Á., Imre K., Kulmala M., (2016a). Regional effect on urban atmospheric nucleation, Atmospheric Chemistry and Physics, 16, 8715–8728.

Salma I., Németh Z., Weidinger T., Kovács B., Kristóf G., (2016b). Measurement, growth types and shrinkage of newly formed aerosol particles at an urban research platform, Atmospheric Chemistry and Physics, 16, 7837–7851.

Scheytt T.J., Freywald J., Ptacek C.J., (2011). Study of selected soil, ground, and surface water samples on perchlorate in Germany: first results. Grundwasser, 16, 37–43.

Seidel D.J., Birnbaum A.N., (2015). Effects of Independence Day fireworks on atmospheric concentrations of fine particulate matter in the United States. Atmospheric Environment, 115, 192–198.

Sun Y., Han Z., Du Z., Li Z., Cong X., (2017). Preparation and performance of environmental friendly Sulphur-Free propellant for fireworks. Applied Thermal Engineering, 126, 987-996.

Temple R.K.G., (2007). The Genius of China: 3,000 Years of Science, Discovery, and Invention (3rd edition). London: André Deutsch, 256–66.

Van Kamp I., Van der Velden P G., Stellato R K., Roorda J., Van Loon J., Kleber R J., Gersons B. B. R., Lebret E. (2006). Physical and mental health shortly after a disaster: first results from the Enschede firework disaster study. European Journal of Public Health, 16, 252-258.

Vecchi R., Bernardoni V., Cricchio D., D'Alessandro A., Fermo P., Lucarelli F., Nava S., Piazzalunga A., Valli G., (2008). The impact of fireworks on airborne particles. Atmospheric Environment, 42, 1121–1132.

Verougstraete V., Lison D., Hotz P., (2003). Cadmium, lung and prostate cancer: A systematic review of recent epidemiological data. Journal of Toxicology Environmental Health, 6, 227–55.

Wang Y., Zhuang G., Xu C., An Z., (2007). The air pollution caused by the burning of fireworks during the lantern festival in Beijing. Atmospheric Environment, 41, 417–431.

Wehner B., Weidensohler A., Heintzenberg, J., (2000). Sub micrometer aerosol size distributions and mass concentrations of the millennium fireworks 2000 in Leipzig, Germany. Journal of Aerosol Science, 31, 1489–1493.

Wen L., Chen J., (2013). Severe aerosol pollution derived from fireworks: a case in Jinan, China. JSM Environmental Science & Ecology, 1, 1004.

Werret S., (2010). Fireworks: Pyrotechnic Arts and Sciences in European History. University of Chicago Press, 1.

WHO, (2021). Global air quality guidelines. Particulate matter (PM2.5 and PM10), ozone, nitrogen dioxide, sulfur dioxide and carbon monoxide. Executive summary. Geneva: World Health Organization, License: CC BY–NC–SA 3.0 IGO.

Wiedensohler A., Birmili W., Nowak A., Sonntag A., Weinhold K., Merkel M., Wehner B., Tuch T., Pfeifer S., Fiebig M., Fjäraa A. M., Asmi E., Sellegri K., Depuy R., Venzac H., Villani P., Laj P., Aalto P., Ogren J. A., Swietlicki E., Williams P., Roldin P., Quincey P., Hüglin C., Fierz–Schmidhauser R., Gysel M., Weingartner E., Riccobono F., Santos S., Grüning C., Faloon K., Beddows D., Harrison R., Monahan C., Jennings S. G., O'Dowd C. D., Marinoni A., Horn H.–G., Keck L., Jiang J., Scheckman J., McMurry P. H., Deng Z., Zhao C. S., Moerman M., Henzing B., de Leeuw G., Löschau G., Bastian S., (2012). Mobility particle size spectrometers: harmonization of technical standards and data structure to facilitate high quality long–term observations of atmospheric particle number size distributions, Atmospheric Measurement Techniques, 5, 657–685.

Yadav S.K., Kumar M., Sharma Y., (2019). Temporal evolution of submicron particles during extreme fireworks. Environmental Monitoring and Assessment, 191, 576.

Yao L., Wang D., Fu Q., Qiao L., Wang H., Li L., Sun W., Li Q., Wang L., Yang X., Zhao Z., Kan H., Xian A., Wang G., Xiao H., Chen J., (2019). The effects of firework regulation on air quality and public health during the Chinese Spring Festival from 2013 to 2017 in a Chinese megacity. Environment International, 126, 96–106.

Zhang J., Huang, X., Chen Y., Luo B., Luo J., Zhang W., Yang F., (2019). Characterization of lead-containing atmospheric particles in a typical basin city of China: Seasonal variations, potential source areas, and responses to fireworks. Science of the Total Environment, 661, 354–363.

Zhang M., Wang X., Chen J., Cheng T., Wang T., Yang X., Chen C., (2010). Physical characterization of aerosol particles during the Chinese New Year's firework events. Atmospheric Environment, 44, 5191–5198.

Zhao S., Yu Y., Yin D., He J., (2017). Effective density of submicron aerosol particles in a typical valley city, western China. Atmospheric Pollution Research, 17, 1–13.

Effects of fireworks on the air quality in Budapest

Felipe Reis Fernandes, MSc Student

Supervisor: Dr. Salma Imre professor

ELTE Department of Analytical Chemistry

Every year on 20th of August a celebration of Saint Stephen's day takes place in Budapest, Hungary. The event includes a massive fireworks spectacle in the central part of the city along the Danube riverbank. The burning of fireworks has the potential of producing aerosols which can have an impact on human health. The characterization of the aerosols produced by such events are mostly centered on the identification of particles containing the metal ions commonly utilized during firework manufacturing process as well as on the particle mass concentration (Yadav et al., 2019). The goal of this work was to approach the aerosol characterization from the perspective of the particle number count and the size distribution given the unique characteristics of the event as well as the opportunity of having more controlled time and space distribution for this occasion in Budapest. The data analyzed has been collected from the time of the celebration on each of the following years: 2009, 2014, 2015, 2016, 2017, 2020 and 2021.

The measurements were done in the Budapest platform for Aerosol Research and Training (BpART) Laboratory with a differential mobility particle sizer (DMPS) for measurement of particles from 6 to 1000 nm divided in 30 distinct size slots as well as a separated Condensation Particle Counter (CPC) for total particle count. Besides the aerosol concentrations, meteorological conditions for wind speed, wind direction, temperature and relative humidity were also collected considering the possible influence of such factors on aerosol measurements.

The results have shown a considerable increase in total aerosol concentration of up to four-fold for the year with the biggest firework event registered from the time series (2021). The most significant increase in mean particle concentration of up to eighteen-fold was detected for the year 2021 for particles ranging from 100-1000 nm. The increase of this fraction seemed to be related to the intensity of the event more than any other fraction and the fireworks had shown a particular distribution of particle size relative concentration compared to the background aerosol levels. The statistical analysis of the data evidenced a natural difference between the means of particle concentration between the one-hour interval before, during and after the fireworks. Despite this natural tendency, fireworks modified the data ranges and central tendency and clearly affected the background particle size distribution of the aerosols.

In any case, on 2009 and 2021, the fireworks seem to have generated enough particles to reach concentration levels dangerous to human health. Further measurements as well as the use of drones, scattered sensors for capturing the event characteristics or even the adoption of the metal ion characterizations contribute to better understanding the characteristics of these events in the future.